Laser-Induced Backside Wet Etching Employing Green DPSS Laser and Liquid Metallic Absorber

Tadatake SATO[*1], Yoshizo KAWAGUCHI[*1], Ryozo KUROSAKI[*1], Aiko NARAZAKI[*1], Wataru WATANABE[*1] and Hiroyuki NIINO[*1]

[*1] *Electronics and Photonics Research Institute, National Institute of Advanced Industrial Science and Technology (AIST), Tsukuba Central 5, 1-1-1 Higashi, Tsukuba, Ibaraki 305-8565, Japan*
E-mail: sato-tadatake@aist.go.jp

An indirect laser processing, laser-induced backside wet etching (LIBWE) is one of effective techniques for flexible laser-direct-write (LDW) type micromachining of transparent materials. Micromachining by LIBWE employing a diode-pumped solid state (DPSS) green laser and a galvanometer-based point scanning system was examined with employing organic dye solution and liquid metal as laser-absorbing media. LIBWE using liquid metal absorber showed smaller threshold pulse energies for etching (9.1 μJ/pulse) than that using organic dye solution (33 μJ/pulse). Different morphologies of etched surfaces were observed for different laser-absorbing media, indicating different mechanisms involved in the etching processes. The laser-induced dynamic phenomena were investigated by means of transient reflection measurements. The different contribution of direct and indirect actions of laser pulses was indicated for LIBWE employing different laser-absorbing media.

DOI:10.2961/jlmn.2011.03.0006
Keywords: Laser direct write, Laser-micromachining, transparent materials, LIBWE

1. Introduction

Towards flexible fabrication of components for micro electro-optical-mechanical system (MEOMS) and microfluidic devices, several techniques for laser micromachining of glass materials have been proposed. Among them, indirect processing methods have been proved to be effective means for precise and low-damage micromachining of hard and brittle transparent materials. In these methods, backside irradiation layout is generally employed. A laser-induced backside wet etching (LIBWE) is one of the promising techniques, that employs liquid laser-absorbing media [1–28]. In addition to machining technique based on a mask-projection system, flexible laser-direct-write (LDW) type machining employing a diode-pumped solid state (DPSS) UV laser with a kHz repetition rate and a galvanometer-based point scanning system was reported as far [6]. Owing to the flexibility, laser marking on the transparent materials would be one of the promising applications of this technique.

As far, various dye solutions, such as pyrene / acetone [1,6,7,9,10,17–19,21,24], pyrene / tetrahydrofuran (THF) [2,18], pyrene / tetrachloroethylene [9,11], pyrene / cyclo-hexane [9], pyrene / toluene [10,11,14–16], pyrene / halo-genated aromatics [14], pyranine / water [3], naphtha-lenetrisulfonic acid sodium salt / water [4], naphthalene / methyl methacrylate [20–22], phenolphthalein/N-methyl-2-pyrrolidone [27], and pure toluene [5,8,13,28], have been used in conjunction with irradiation with UV lasers. On the other hand, LIBWE employing green laser (λ= 532 nm) was first reported by Cheng et al.: they used rose bengal saturated acetone solution as a liquid laser absorber [25].

Laser machining using inorganic solution has been reported by Schafeev and co-workers [29–31]; in this method, metal layer deposit by the laser irradiation contributes for the surface etching. Recently, similar approach was reported by Hong and co-workers [32].

Liquid metallic absorber (Ga) for LIBWE was first examined by Zimmer and co-workers, showing extremely high etch rate as high as 630 nm/pulse [12], in comparison with typical rate of 0.1–40 nm/pulses for LIBWE using dye solutions. The etching with mercury also showed similar high etch rate [13]. Molten tin was used for etching and compared with laser-induced dry etching (LIBDE) using thin film of tin as a laser absorbing medium [23,34]. These works were done in combination with UV excimer laser used for LIBWE with organic dye solution. Meanwhile, metallic absorber allows the employment of lasers for radiation in the IR, VIS range as well as UV range. LIBWE employing liquid metal absorber and NIR laser (λ = 1064 nm) was reported [35,36]. Recently, LIBWE employing green laser and liquid metal absorber was reported. In this work, eutectic indium/gallium was used as an absorber as well as liquid gallium [26]. As the authors argued, visible laser system is far more economical than UV laser systems. Moreover, it can be applied to machining of transparent materials with low transmittance in the UV range.

In this work, micromachining by beam-scanning LIBWE with green DPSS laser was examined. The properties of LIBWE such as the etch rates is dependent on the processing parameters. LIBWE employing organic (O-LIBWE) and liquid metallic laser absorbers (M-LIBWE) were examined and compared under the identical conditions of irradiation.

2. Experimental

Second-harmonic-generated (SHG) pulses of a single-mode diode-pumped solid state (DPSS) laser, a Nd:YVO_4 laser (SpectraPhysics, J80-YHP40, λ = 532 nm, FWHM 35 ns, M^2 < 1.2), were used for LIBWE in ambient conditions. The laser was operated at the repetition rate of 5–40 kHz. The laser beam was expanded by 4 times with a zoom-beam-expander (Sill Optics), and scanned with galvanometer-based point scanning module (GSI Group, XY10M2). Scanned beam was focused by means of a plano-convex lens (f=200 mm).

A fused-silica glass plate (Tosoh SGM Co., ES grade) with a thickness of 2 mm was used as a sample. After the glass sample was mounted at an optimized position on the stage, the sample position was fixed during the laser irradiation with scanning. Rhodamin6G dissolved in ethanol-toluene mixture (v/v = 1/1) with saturated concentration was used as an organic dye solution for LIBWE, while liquid gallium was used as a metallic absorber. When gallium was used, the sample cell was heated to 45 °C.

After etching, the silica glasses on which microtrenches were formed by O-LIBWE were thoroughly rinsed with ethanol to removed remaining dye molecules. While the glasses etched by M-LIBWE were cleaned ultrasonically for 30 min in the diluted hydrochloric acid (2 N), after wiping off gallium attached to the surface by a soft tissue.

Fabricated microstructures were observed by means of a laser confocal microscope (Keyence, VK-8500) or a scanning electron microscope (SEM, Keyence, VK-7800). Depth-profiles of the surface were measured by the laser confocal microscope. As described later, the bottom of etched microtrenches were not smooth. The depths of the microtrenches were evaluated by averaging 91 profiles obtained with a constant interval of ca. 3 μm in the region with a length of 290 μm.

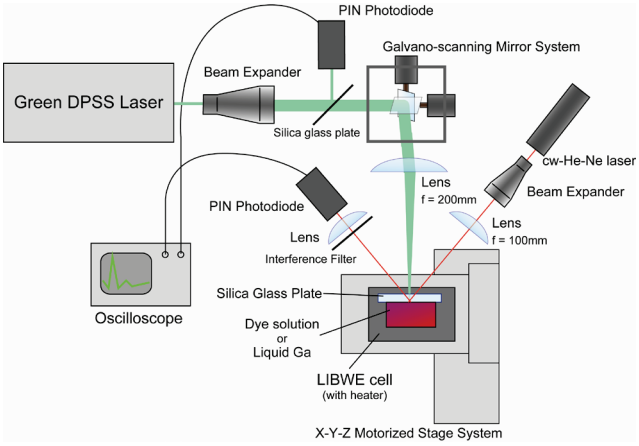

Fig. 1 Experimental setup for beam-scanning LIBWE employing green DPSS laser and transient reflectance measurements.

The schematic drawing of setups for transient reflection measurements is shown in Fig. 1. A continuous wave (cw) helium-neon laser (Melles Griot, 25LHP213, λ = 632.8 nm, 0.5 mW, TEM_{00}, 0.46 mmϕ) was used as a source of probe light. To focus this into smaller area than the focused spot of laser beam for etching, the probe light was expanded by 10 times with beam-expander and then focus by plano-convex lens (f = 100 mm). The calculated diameters of the focused spot of laser beams for etching and probing are 45 and 18 μm, respectively. The reflected probe-light is focused onto a Si pin photodiode with a rise time < 300 ps. A digital storage oscilloscope (Lecroy 9350A) with a sample rate of 1 GS/s was used to record transient reflectance signals. The oscilloscope was triggered by partially-reflected light of laser for etching detected by another Si pin photodiode. Power of probe laser was measured by means of power meter (Laser Check, Sigma Koki).

3. Results and Discussions

3.1 Dependence on pulse energies

Microtrenches were fabricated by LIBWE with pulse repetition of 5 kHz, and focused beam was scanned with a speed of 13.2 mm/s: laser pulses were irradiated with an interval of 2.64 μm/pulse. Scan of the laser beam was repeated 1–9 times.

When organic dye solution was used as a laser-absorbing medium, etching was observed for the higher pulse energies than 36.4 μJ/pulse. Fig. 2 shows the depths of the microtrenches in dependent on the numbers of the repeated scans: applied pulse energy was 43.6 μJ/pulse. Depths of microtrenches increased linearly with numbers of scans. Averaged etch depth for single scan was estimated to be 0.25 μm/scan.

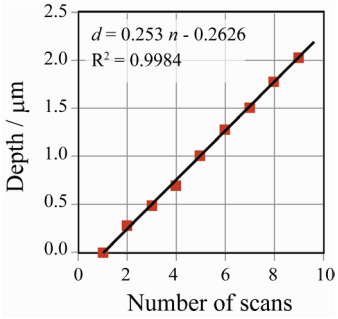

Fig. 2 Depths of the microtrenches fabricated with repeated scans. Applied pulse energy: 43.6 μJ/pulse.

By scanning the laser beam, laser pulses are irradiated with partial overlap. Etch rate under the present conditions were estimated from the equation (1) proposed by Cheng and co-workers [24].

$$R_{\mathrm{etch}} = \frac{d}{\left(2\omega_0 / V\right) \times f_{\mathrm{rep}}} \qquad (1)$$

where d is the etched depth, V is the speed of scanning the laser beam, $2\omega_0$ is the focused beam size and f_{rep} is the pulse repetition rate. A denominator of this equation means effective number of overlapping laser pulses at one point in scanned lines.

In our setup, the laser beam with a diameter of 3.6 mm (after expanded) is focused by lens with a focal length of 200 mm. The size of the focused laser beam spot is calculated to be 45 μm in diameter by equation (2),

$$2\omega_0 = \frac{4\lambda}{\pi} M^2 \left(\frac{F}{D}\right) \qquad (2)$$

where F and D are the focal length of lens and the diameter of laser beam to be focused.

Variations in widths were observed for shallow microtrenches, while those with depths larger than 6 μm showed constant the widths of 27 μm. Therefore, this value was applied to equation (1) as a practical beam size for etching. The effective number of overlapping laser pulses is 9.46 in this case. The widths of the fabricated microtrenches were smaller than the calculated value, probably because of the threshold for etching. From the averaged etch depth for single scan, 0.25 μm/scan, etch rate was estimated to be 24 nm/pulse. Thus evaluated etch rates for O- and M-LIBWE are shown in Fig. 3.

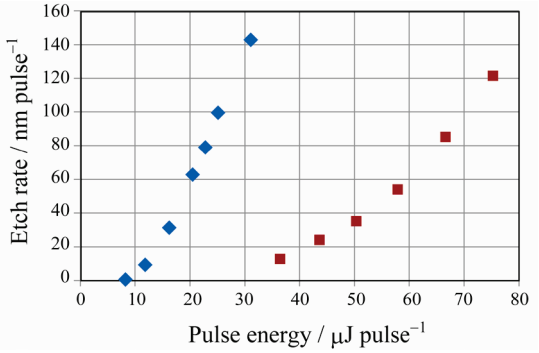

Fig. 3 Etch rates of silica glass in dependence of pulse energy obtained for (square) O- and (diamond) M-LIBWE.

When liquid gallium was used, etching was observed for the higher pulse energies than 8.2 μJ/pulse. Microtrenches with widths up to 25 μm were obtained: this width was used to evaluate etch rate. Threshold pulse energies for etching were estimated to be 9.1 and 33 μJ/pulse, respectively. For the respective practical beam size, these values correspond to 1.9 and 5.7 J/cm^2. At the present conditions, threshold evaluated for M-LIBWE was lower than that of O-LIBWE despite high reflectivity at glass-gallium interface.

The threshold value evaluated for M-LIBWE was higher than the reported value (488 mJ/cm^2) [26]. This difference would be due to the feature size. On the other hand, the threshold obtained for O-LIBWE is similar with that reported by Cheng [25], although they used different solution.

Zimmer et al. argued that the major difference between O- and M-LIBWE was the existence of incubation effect [11,37]. In Fig. 2, the depth of the microtrench fabricated with single scan is zero, meaning no trench was fabricated. When applied pulse energy is low, the etching was observed from the second scan. Formation of the trench from the first scan was observed with the pulse energies higher than 58.0 μJ/pulse. On the contrary, etching was discerned from the first scan in M-LIBWE. The incubation process is inadequate for O-LIBWE under the present conditions.

3.2 Morphology of etched surface

Apart from energies required for etching, different surface morphology of etched area was shown by laser-absorbing media. Fig. 4 shows SEM images of microtrenches fabricated by O- and M-LIBWE under the conditions showing almost similar etch rates. Under these conditions, the surface of the etched area was not smooth as shown in the figures. It is different from the previous reports [25]. The reason for non-smooth surface would be mainly ascribed to the conditions of laser-beam scanning: too high scan-speed resulting in low pulse overlap. Thus the microstructures fabricated under the present conditions could not be applied to microoptics or microfluidics, but it could be used for laser marking. The surface quality could be improved by optimizing the conditions such as scan-speed, pulse repetition, laser-absorbing media, and so on.

On the surface obtained by O-LIBWE, ripple-like structure was observed (Fig. 4(a)). The interval of the structure was ca. 2.3 μm, almost similar with the interval of irradiated pulses. The difference in depth by the ripple-like structure was about 1 μm. The observed structure might be the similar one to the reported surface features related to rapid resolidification after melting [37]. On the other hand, the surface obtained by etching with liquid gallium was relatively smooth, indicating high melting depths in this case [12].

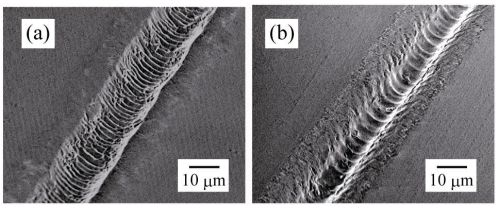

Fig. 4 SEM images of microtrenches fabricated by (a) O- and (b) M-LIBWE. Conditions for fabrication: (a) pulse energy: 67 μJ/pulse, 5 scan; depth: 3.6 μm, (b) pulse energy: 23 μJ/pulse, 5 scan; depth: 4.0 μm.

Moreover, as Fig. 4 shows, the edges of the microtrench fabricated by O-LIBWE were sharp in comparison with those fabricated by M-LIBWE. Averaged depth-profiles of the cross-sections of microtrenches are shown in Fig. 5. The depth-profile for M-LIBWE shows keen Gaussian-like shape together with rim structures with height of 90–150 nm (Fig. 5(b)), while that by O-LIBWE shows relatively round bottom and small rim structures.

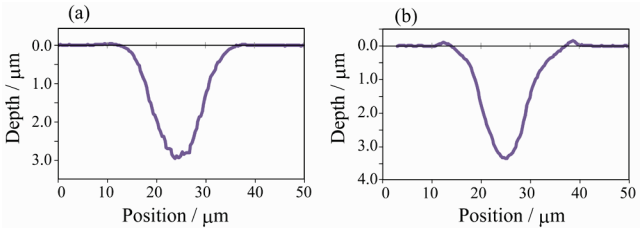

Fig. 5 Averaged depth-profiles of the cross-sections of microtrenches fabricated by (a) O- and (b) M-LIBWE.

Observed different morphology of the etched surface would indicate the different mechanisms involved in the etching processes. Fig. 6 shows top-view images of microtrenches obtained by means of laser confocal

microscope. Fig. 6(b) clearly shows overlapping circles indicating the shape of laser spots. Therefore, this image indicates the major contribution of direct actions of focused laser beam to M-LIBWE. On contrary, the shape of laser spot was indiscernible in Fig 6(a), indicating that the contribution of direct actions of focused laser beam is minor in this case. Instead the indirect actions, that is, the actions by laser-heated liquid, would be important in O-LIBWE.

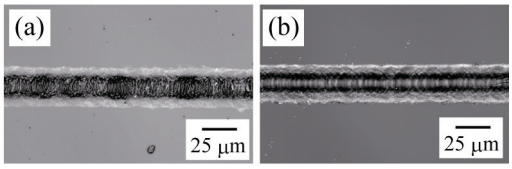

Fig. 6 Top-view images of microtrenches fabricated by (a) O-LIBWE and (b) M-LIBWE.

3.3 Dependence on pulse repetition rate

Fig. 7 shows the dependence of etch rate on pulse repetition rate, expressed as relative changes from the etch rate obtained at pulse repetition of 5 kHz are shown. Pulse energies for etching were set to 67 and 23 μJ/pulse, for O- and M-LIBWE, respectively: etch rates were respective shown to be 86 and 80 nm/pulse at the pulse repetition rate of 5 kHz. In both cases, with increasing pulse repetition rate, etch rates decreased as shown in Fig. 7. Etch rates of O-LIBWE decreased in the range of the repetition rate up to 25 kHz. At the pulse repetition rates higher than 25 kHz, etch rate became constant at the rate of ca. 22 % of the original one (86 nm/pulse at 5 kHz). Meanwhile, the etch rates of M-LIBWE reached to the rate of ca. 50 % of the original one (80 nm/pulse at 5 kHz) at 30 kHz.

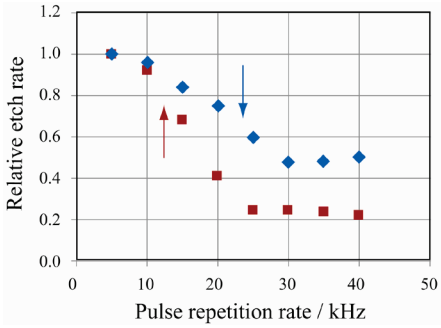

Fig. 7 Relative etch rates of silica glass in dependence of pulse repetition rate obtained for (square) O- and (diamond) M-LIBWE. Arrows pointing up and down indicate the lifetime of transient change in reflection observed for O- and M-LIBWE.

In the O-LIBWE, glass-liquid interface was transiently lost by generation of cavitation bubble [5]. This should be one reason for observed decrease in etch rate at high pulse repetition rate. In this work, the dynamics of the cavitation bubble was investigated by means of transient reflection measurement as previously reported for the LIBWE using excimer laser and organic dye solution [13]. Obtained transient reflection signals are shown in Fig. 8.

Steady reflectance of probe laser was measured to be 13 and 82 % for the interfaces of glass/organic dye solution and glass/liquid gallium, respectively. In the case of O-LIBWE, the reflectivity is temporally increased by the generation of cavitation bubble with lower density (Fig. 8(a)). The lifetime of cavitation bubble was evaluated to be 78 μs for irradiation at 67 μJ/pulse. On the other hand, temporal reduction of reflection was observed in the case of M-LIBWE as shown in Fig. 8(b). Observed transient signals should be ascribed to temporal change of the glass-metal interface probably due to the generation of cavitation bubble as described later. The lifetime of the phenomena was measured to be 45μs for irradiation at 23 μJ/pulse. Observed lifetime of cavitation bubble in O-LIBWE (78 μs) corresponds to the repetition of 12.8 kHz, while 45 μs obtained for M-LIBWE corresponds 23.3 kHz: these are indicated in Fig. 7. The lifetime of cavitation bubble in O-LIBWE located early stage of decreasing in etch rate, indicating that the existence of glass-liquid interface is important for this process. Meanwhile, it for M-LIBWE located to later stage of decreasing, indicating that the observed phenomena is not major origin of observed decrease in etch rate.

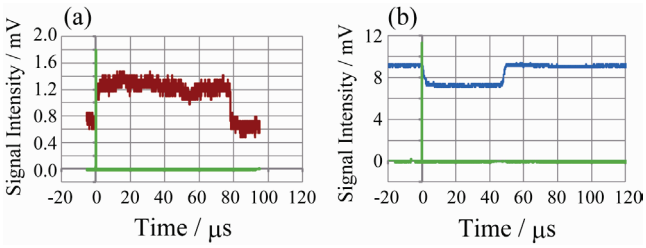

Fig. 8 Transient reflection signals observed for (a) O- and (b) M-LIBWE with pulse energies of 67 and 23 μJ/pulse, respectively.

It was argued that one advantage of M-LIBWE is high boiling point of gallium (T_B = 2200 °C), which permits melting of fused silica without liquid evaporation [37]. Observed transient change in reflection might indicate the temporal loss of the glass-liquid interface by generation of cavitation bubble. The observed change in signal seems too small for the interface between glass and vapor. Observed small change might be ascribed to generation of plasma in the bubble. As an indirect laser machining technique, laser-induced plasma-assisted ablation (LIPAA) process was proposed by Zhang and co-workers [38]. In this process, plasma generated by laser ablation of metal contributes to generate electron excitation acting as absorption sites at the surface of glass [39]. In M-LIBWE, similar action of laser generated plasma would be possible. The LIPAA process can be operated with narrow gap (less than 100 μm) between metal and glass. As shown earlier, in M-LIBWE direct action of laser pulse is more important in comparison with the case of O-LIBWE. Therefore, in M-LIBWE, the mechanism similar to LIPAA would be dominant for etching. On the other hand, the indirect action of heated liquid would be more important factor in O-LIBWE.

4. Conclusions

Micromachining by LIBWE employing a diode-pumped solid state (DPSS) green laser and a galvanometer-based point scanning system was examined with employing organic dye solution and liquid metal as laser-absorbing media. LIBWE using liquid metal absorber showed smaller

threshold pulse energies for etching (9.1 μJ/pulse) than that using organic dye solution (33 μJ/pulse). Different morphologies of etched surface were observed for different laser-absorbing media, indicating different mechanisms involved in the etching processes. In particular, the clearly discernable traces of laser spots indicated the importance of direct action of laser pulses in M-LIBWE.

The laser-induced dynamic phenomena were investigated by means of transient reflection measurements. The decrease in etch rate with increasing pulse repetition rate and the lifetime of transient reflection showed that the important role of glass-liquid interface in O-LIBWE. Thus, the different contribution of direct actions of laser pulses and indirect actions of laser-heated liquid was indicated for LIBWE employing different laser-absorbing media.

5. Acknowledgements

This work was supported by The Amada Foundation for Metal Work Technology.

References

[1] J. Wang, H. Niino, and A. Yabe: Appl. Phys. A 68 (1999) 111.
[2] J. Wang, H. Niino, A. Yabe: Jpn. J. Appl. Phys. 38 (1999) L761.
[3] X. Ding, Y. Yasui, Y. Kawaguchi, H. Niino, A. Yabe: Appl. Phys. A, 75, (2002) 437.
[4] X. Ding, Y. Kawaguchi, H. Niino, A. Yabe, Appl. Phys. A 75 (2002) 641.
[5] H. Niino, Y. Yasui, X. Ding, A. Narazaki, T. Sato, Y. Kawaguchi, A. Yabe: J. Photochem. Photobiol. A: Chem., 158, (2003) 179.
[6] X. Ding, T. Sato, Y. Kawaguchi, H. Niino: Jpn. J. Appl. Phys., 42, (2003) L176.
[7] Y. Kawaguchi, T. Sato, A. Narazaki, R. Kurosaki, H. Niino: Jpn. J. Appl. Phys., 44, (2005) L176.
[8] H. Niino, Y. Kawaguchi, T. Sato, A. Narazaki, T. Gumpenberger, R. Kurosaki: Appl. Surf. Sci., 252, (2006) 4387.
[9] R. Böhme, A. Braun, K. Zimmer: Appl. Surf. Sci., 196, (2002) 276.
[10] K. Zimmer, A. Braun, R. Böhme: Appl. Surf. Sci., 208-209, (2003) 199.
[11] R. Böhme, K. Zimmer: Appl. Surf. Sci., 247, (2005) 256.
[12] K. Zimmer, R. Böhme, D. Ruthe, B. Raushenbach: Appl. Phys. A, 84, (2006) 455.
[13] R. Böhme, T. Otto, K. Zimmer: Appl. Surf. Sci. 252 (2006) 4392.
[14] R. Böhme, K. Zimmer: Appl. Phys. A, 83 (2006) 9.
[15] K. Zimmer, R. Böhme, D. Ruthe, B. Raushenbach: Appl. Surf. Sci., 253, (2007) 6588.
[16] K. Zimmer, M. Ehrhardt, R. Böhme: J. Appl. Phys., 107, (2010) 034908.
[17] G. Kopitkovas, T. Lippert, C. David, S. Canulescu, A. Wokaun, J. Gobrecht: Micloelectron. Eng., 67-68, (2003) 438.
[18] G. Kopitkovas, T. Lippert, C. David, S. Canulescu, A. Wokaun, J. Gobrecht, J. Photochem. Photobiol. A: Chem. 166 (2004) 135.
[19] G. Kopitkovas, V. Deckert, T. Lippert, F. Raimondi, C. W. Schneider, A. Wokaun: Phys. Chem. Chem. Phys., 10, (2008) 3195.
[20] C. Vass, T. Smausz, B. Hopp: J. Phys. D: Appl. Phys., 37, (2004) 2449.
[21] Cs. Vass, D. Sebok, B. Hopp, Appl. Surf. Sci. 252 (2006) 4768.
[22] C. Vass, K. Osvay, T. Veso, B. Hopp, Z. Bor: Appl. Phys. A 93, (2008) 69.
[23] B. Hopp, T. Smausz, T. Csizmadia, C. Vass, T. Csako, G. Szabo: J. Laser Micro/Nanoeng., 5, (2010) 80.
[24] J.-Y. Cheng, M.-H. Yen, C.-W. Wei, Y.-C. Chuang, T.-H. Young, J. Micromech. Microeng. 15 (2005) 1147.
[25] J.-Y. Cheng, M.-H. Yen, T.-H. Young: J. Micromech. Microeng. 16, (2006) 2420.
[26] M.-H. Yen, C.-W. Huang, W.-C. Hsu, T.-H. Young, K. Zimmer, J.-Y. Cheng: Appl. Surf. Sci., 257, (2010) 87.
[27] K. Fujito, T. Hashimoto, K. Samonji, J. S. Speck, S. Nakamura: J. Cryst. Growth, 272, (2004) 370.
[28] T. Lee, D. Jang, D. Ahn, D. Kim: J. Appl. Phys., 107, (2010) 033112.
[29] S. I. Dolgaev, A. A. Lyalin, A. V. Simakin, G. A. Shafeev: Quantum Electron., 26, (1996) 65.
[30] S. I. Dolgaev, A. A. Lyalin, A. V. Simakin, G. A. Shafeev: Appl. Surf. Sci., 96-98, (1996) 491.
[31] A. V. Simakin, E. N. Lonbin, G. A. Shafeev, Quantum Electron. 30, (2000), 263.
[32] Z. Q. Huang, M. H. Hong, T. B. M. Do, Q. Y. Lin: Appl. Phys. A: 93, (2008) 159.
[33] K. Zimmer, R. Böhme, D. Hirsch, B. Rauschenbach: J. Phys. D: Appl. Phys., 39, (2006) 4651.
[34] B. Hopp, T. Smausz, C. Vass, G. Szabo, R. Böhme, D. Hirsch, K. Zimmer: Appl. Phys. A, 94, (2009) 899.
[35] K. Zimmer, R. Böhme, S. Pissadakis, L. Hartwig, G. Reisse, B. Raushenbach: Appl. Surf. Sci., 253, (2006) 2796.
[36] K. Zimmer, R. Böhme, B. Raushenbach: Appl. Phys. A, 86, (2007) 409.
[37] R. Böhme, K. Zimmer: Appl. Surf. Sci., 253, (2007) 8091.
[38] J. Zhang, K. Sugioka, K. Midorikawa: Appl. Phys. A, 67, (1998) 545.
[39] Y. Hanada, K. Sugioka, K. Obata, S.V. Garnov, I. Miyamoto, K. Midorikawa: J. Appl. Phys., 99, (2006) 043301.

(Received: June 06, 2011, Accepted: November 03, 2011)